Theoretical model for diffuse optical wave scattering from a three-dimensional slab bounded by randomly rough surfaces

Gérard Berginc, Claude Bourrely

▶ To cite this version:

HAL Id: hal-00136114

https://hal.science/hal-00136114

Submitted on 12 Mar 2007

Theoretical Model for Diffuse Optical Wave Scattering from a Three-Dimensional Slab Bounded by Randomly Rough Surfaces

Gérard Berginc[1] and Claude Bourrely[2]

[1]Thalès Optronique, BP 55, 78233 Guyancourt Cedex, France.
gerard.berginc@fr.thalesgroup.com

[2]Centre de Physique Théorique[3], CNRS-Luminy Case 907
13288 Marseille Cedex 9, France.
claude.bourrely@cpt.univ-mrs.fr

Abstract

Our purpose is to show how light can interact with slab bounded by rough surfaces. In this paper, we consider three-dimensional structures bounded by two-dimensional weakly rough surfaces or by two-dimensional randomly rough surfaces with small-slope. We discuss the extension of the small-slope approximation method to slabs with two randomly rough surfaces. The fourth order terms of the perturbative development are required in order to take into account the interactions between the randomly rough surfaces.

keywords: scattering by random slabs, rough surface, small-slope approximation.

---

3. Unité Mixte de Recherche 6207 du CNRS et des Universités Aix-Marseille I, Aix-Marseille II et de l'Université du Sud Toulon-Var - Laboratoire affilié la FRUMAM.

Theoretical Model for Diffuse Optical Wave Scattering from a Three-Dimensional Slab Bounded by Randomly Rough Surfaces

Gérard Berginc[1] **and Claude Bourrely**[2]

[1]Thalès Optronique, BP 55, 78233 Guyancourt Cedex, France.

gerard.berginc@fr.thalesgroup.com

[2]Centre de Physique Théorique[3], CNRS-Luminy Case 907

13288 Marseille Cedex 9, France.

claude.bourrely@cpt.univ-mrs.fr

Abstract Our purpose is to show how light can interact with slab bounded by rough surfaces. In this paper, we consider three-dimensional structures bounded by two-dimensional weakly rough surfaces or by two-dimensional randomly rough surfaces with small-slope. We discuss the extension of the small-slope approximation method to slabs with two randomly rough surfaces. The fourth order terms of the perturbative development are required in order to take into account the interactions between the randomly rough surfaces.

keywords: scattering by random slabs, rough surface, small-slope approximation.

1. Introduction

Volume and surface scattering is a topic, which has been studied in an extensive way in different domains such as radio-physics, geophysical remote sensing and surface optics. In this paper, we study structures with two-dimensional randomly rough surfaces, including scattering from freestanding films or films deposited on metal. We present the extension of the small-slope approximation method to slabs with rough interfaces based upon the fourth order term of the perturbative development.

2. Scattering Amplitude

A.G. Voronovich [1,2] observed that if the boundary of a rough surface $z = h(r)$ (see Fig. 1) is shifted by a horizontal distance d, the scattering amplitude (SA) transforms as:

$$\overline{\boldsymbol{R}}_{\boldsymbol{x}\to h(\boldsymbol{x}-\boldsymbol{d})}(\boldsymbol{p}|\boldsymbol{p}_0) = \exp^{-i(\boldsymbol{p}-\boldsymbol{p}_0)\cdot\boldsymbol{d}} \, \overline{\boldsymbol{R}}_{\boldsymbol{x}\to h(\boldsymbol{x})}(\boldsymbol{p}|\boldsymbol{p}_0)\,, \tag{1}$$

while for a vertical shift by H we obtain:

$$\overline{\boldsymbol{R}}_{h+H}(\boldsymbol{p}|\boldsymbol{p}_0) = \exp^{-i(\alpha_0(\boldsymbol{p})+\alpha_0(\boldsymbol{p}_0))\,H} \, \overline{\boldsymbol{R}}_h(\boldsymbol{p}|\boldsymbol{p}_0)\,, \tag{2}$$
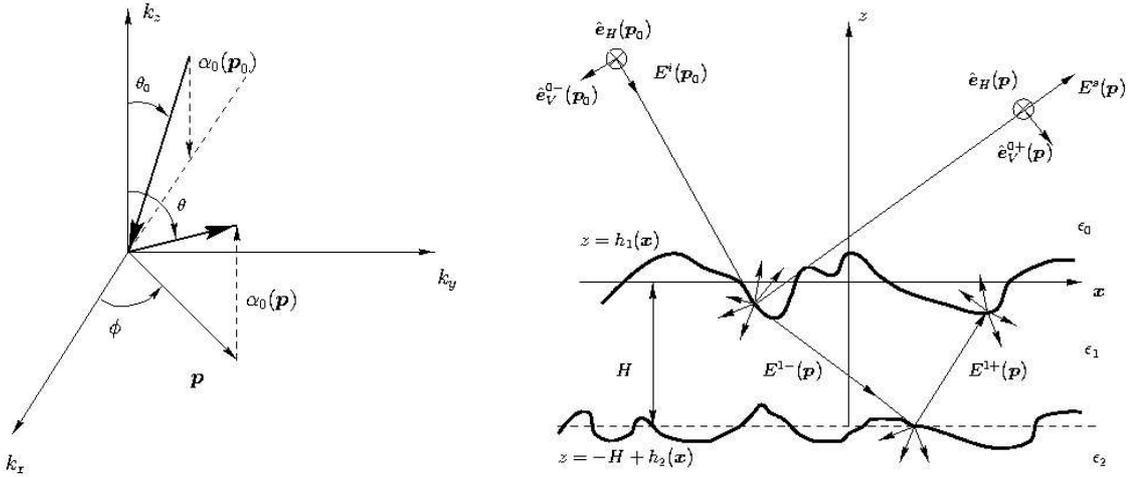
FIG. 1. *Definition of the randomly rough slab. Notations:* $\boldsymbol{k}_{\boldsymbol{p}_0}^- \equiv \boldsymbol{p}_0 - \alpha_0(\boldsymbol{p}_0)\hat{\boldsymbol{e}}_z$, $\alpha_0(\boldsymbol{p}_0) \equiv (\epsilon_0 K_0^2 - \boldsymbol{p}_0^2)^{\frac{1}{2}}$, $\boldsymbol{k}_{\boldsymbol{p}}^\pm \equiv \boldsymbol{p} \pm \alpha_0(\boldsymbol{p})\hat{\boldsymbol{e}}_z$, $\alpha_0(\boldsymbol{p}) \equiv (\epsilon_0 K_0^2 - \boldsymbol{p}^2)^{\frac{1}{2}}$.

from these properties he postulated an expression of the scattering amplitude in a form given by:

$$\overline{R}(\boldsymbol{p}|\boldsymbol{p}_0) = \int \mathrm{d}^2\boldsymbol{x}_s \, \exp^{-\mathrm{i}\,(\boldsymbol{p}-\boldsymbol{p}_0)\cdot\boldsymbol{x}_s - \mathrm{i}(\alpha_0(\boldsymbol{p})+\alpha_0(\boldsymbol{p}_0))\,h(\boldsymbol{x}_s)} \, \overline{\boldsymbol{\varphi}}(\boldsymbol{p},\boldsymbol{p}_0,\boldsymbol{x}_s)\,. \tag{3}$$

A large amount of literature has been devoted to study further developments of this method (see for example [3,4]). In a previous work [5], we developed the small-amplitude method to the case of a layer delimited by weakly rough surfaces. In Ref. [6], we compared the small-amplitude method, the small-slope approximation with experimental results. In the following, we will consider a theoretical model based upon the small-slope approximation for the case of a layer delimited by two rough surfaces. A natural extension of the scattering amplitude involving two rough surfaces reads in Fourier space:

$$\begin{aligned}
\overline{R}(\boldsymbol{p},\boldsymbol{p}_0) &= \int d^2\boldsymbol{r}\,d^2\boldsymbol{r}' \frac{d^2\boldsymbol{\xi}}{(2\pi)^2} \frac{d^2\boldsymbol{\xi}'}{(2\pi)^2} \\
&\quad \exp\left[-i(\boldsymbol{p}-\boldsymbol{p}_0-\boldsymbol{\xi})\cdot\boldsymbol{r} - i(\boldsymbol{p}-\boldsymbol{p}_0-\boldsymbol{\xi}')\cdot\boldsymbol{r}' - i(\alpha(\boldsymbol{p})+\alpha(\boldsymbol{p}_0))(h_1(\boldsymbol{r})+h_2(\boldsymbol{r}'))\right] \\
&\quad \times \tilde{\boldsymbol{\Phi}}\left[\boldsymbol{p},\boldsymbol{p}_0;\, \boldsymbol{\xi};\, \boldsymbol{\xi}';\, [h_1(\boldsymbol{\xi})];\, [h_2(\boldsymbol{\xi}')]\right]\,,
\end{aligned} \tag{4}$$

here, $h_1(\boldsymbol{\xi})$ and $h_2(\boldsymbol{\xi})$ are the Fourier transforms of the roughness of the different surfaces.

In this paper, we consider a three-dimensional structure with two rough surfaces and the scattering amplitude is expanded in a perturbative development:

$$\overline{R} = \overline{R}^{(00)} + \overline{R}^{(10)} + \overline{R}^{(01)} + \overline{R}^{(11)} + \overline{R}^{(20)} + \overline{R}^{(21)} + \overline{R}^{(12)} + \overline{R}^{(22)} + \overline{R}^{(30)} + \overline{R}^{(03)} + \ldots\,, \tag{5}$$

$\overline{R}^{(nm)}$ contains powers of $h_1^n h_2^m$, in order to take into account the interaction between the two surfaces.

Following the method proposed by Voronovich we expand the functional $\tilde{\boldsymbol{\Phi}}$ in the form of

3

a Taylor series:

$$\tilde{\boldsymbol{\Phi}}(\boldsymbol{p},\boldsymbol{p}_0,\boldsymbol{\xi},\boldsymbol{\xi}') = \sum_{nm,i_1\ldots i_p} \int d^2\boldsymbol{\xi}_1\ldots d^2\boldsymbol{\xi}_p \delta(\boldsymbol{\xi}-\boldsymbol{\xi}_1-\ldots\boldsymbol{\xi}_p)\tilde{\boldsymbol{\Phi}}^{(nm)i_1..i_p}(\boldsymbol{\xi}_1\ldots\boldsymbol{\xi}_p)h_1(\boldsymbol{\xi}_1)\ldots h_2(\boldsymbol{\xi}_p),$$

(6)

where we have truncated the series up to fourth order. $\tilde{\boldsymbol{\Phi}}^{(nm)i_1..i_p}(\boldsymbol{\xi}_1.....\boldsymbol{\xi}_p)$ represent the 14 unknown kernel functions, we have to determine for this structure.

From gauge transformations we can derive an important relation between the orders n - 1; n; n + 1, namely:

$$\tilde{\boldsymbol{\Phi}}^{(nm)} = [\tilde{\boldsymbol{\Phi}}^{(nm)} - \tilde{\boldsymbol{\Phi}}^{(nm)}\big|_{\boldsymbol{\xi}_n=\boldsymbol{p}-\boldsymbol{p}_0-\boldsymbol{\xi}_1-\cdots-\boldsymbol{\xi}_{n-1}}] + \tilde{\boldsymbol{\Phi}}^{(nm)}\big|_{\boldsymbol{\xi}_n=\boldsymbol{p}-\boldsymbol{p}_0-\boldsymbol{\xi}_1-\cdots-\boldsymbol{\xi}_{n-1}},$$

(7)

As an example of order 2 in the above series we obtain:

$$\int \frac{d^2\boldsymbol{p}_1}{(2\pi)^2}\left[-\frac{(\alpha_0(\boldsymbol{p})+\alpha_0(\boldsymbol{p}_0))^2}{2}(\tilde{\boldsymbol{\Phi}}_u^{(0)}(\boldsymbol{p},\boldsymbol{p}_0)+\tilde{\boldsymbol{\Phi}}_d^{(0)}(\boldsymbol{p},\boldsymbol{p}_0))\right.$$

$$\left.+\tilde{\boldsymbol{\Phi}}^{(11)12}(\boldsymbol{p},\boldsymbol{p}_0,\boldsymbol{p}-\boldsymbol{p}_1,\boldsymbol{p}_1-\boldsymbol{p}_0)\right]h_1(\boldsymbol{p}-\boldsymbol{p}_1)h_2(\boldsymbol{p}_1-\boldsymbol{p}_0)$$

$$+\int \frac{d^2\boldsymbol{p}_1}{(2\pi)^2}\left[-\frac{(\alpha_0(\boldsymbol{p})+\alpha_0(\boldsymbol{p}_0))^2}{2}(\tilde{\boldsymbol{\Phi}}_u^{(0)}(\boldsymbol{p},\boldsymbol{p}_0)+\tilde{\boldsymbol{\Phi}}_d^{(0)}(\boldsymbol{p},\boldsymbol{p}_0))\right.$$

$$\left.+\tilde{\boldsymbol{\Phi}}^{(11)21}(\boldsymbol{p},\boldsymbol{p}_0,\boldsymbol{p}-\boldsymbol{p}_1,\boldsymbol{p}_1-\boldsymbol{p}_0)\right]h_2(\boldsymbol{p}-\boldsymbol{p}_1)h_1(\boldsymbol{p}_1-\boldsymbol{p}_0)$$

$$+\int \frac{d^2\boldsymbol{p}_1}{(2\pi)^2}\left[-\frac{(\alpha_0(\boldsymbol{p})+\alpha_0(\boldsymbol{p}_0))^2}{2}\tilde{\boldsymbol{\Phi}}_u^{(0)}(\boldsymbol{p},\boldsymbol{p}_0)\right.$$

$$\left.+\tilde{\boldsymbol{\Phi}}^{(20)}(\boldsymbol{p},\boldsymbol{p}_0,\boldsymbol{p}-\boldsymbol{p}_1,\boldsymbol{p}_1-\boldsymbol{p}_0)\right]h_1(\boldsymbol{p}-\boldsymbol{p}_1)h_1(\boldsymbol{p}_1-\boldsymbol{p}_0)$$

$$+\int \frac{d^2\boldsymbol{p}_1}{(2\pi)^2}\left[-\frac{(\alpha_0(\boldsymbol{p})+\alpha_0(\boldsymbol{p}_0))^2}{2}\tilde{\boldsymbol{\Phi}}_d^{(0)}(\boldsymbol{p},\boldsymbol{p}_0)\right.$$

$$\left.+\tilde{\boldsymbol{\Phi}}^{(02)}(\boldsymbol{p},\boldsymbol{p}_0,\boldsymbol{p}-\boldsymbol{p}_1,\boldsymbol{p}_1-\boldsymbol{p}_0)\right]h_2(\boldsymbol{p}-\boldsymbol{p}_1)h_2(\boldsymbol{p}_1-\boldsymbol{p}_0).$$

(8)

3. Computation of the kernel functions

For each order of the small-slope approximation the functions $\tilde{\boldsymbol{\Phi}}^{(nm)}$ are indentified with $\tilde{\boldsymbol{X}}^{(nm)}$ obtained from the small-amplitude perturbation method described in Ref. [5].

For instance, $\tilde{\boldsymbol{\Phi}}^{(12)221}$ describes the interaction of the electromagnetic field once with the upper surface and twice with the lower surface in the order 2-2-1.
We have:

$$\tilde{\boldsymbol{\Phi}}^{(12)221}(\boldsymbol{p},\boldsymbol{p}_0,\boldsymbol{\xi}_1,\boldsymbol{\xi}_2,\boldsymbol{\xi}_3) = \frac{\mathrm{i}\,\alpha_0(\boldsymbol{p}_0)}{\alpha_0(\boldsymbol{p})+\alpha_0(\boldsymbol{p}_0)}\Big\{$$

$$\frac{1}{5}\left[\overline{\boldsymbol{X}}^{(22)1221}+\overline{\boldsymbol{X}}^{(22)2121}+\overline{\boldsymbol{X}}^{(22)2211}+\overline{\boldsymbol{X}}^{(13)2221}+\overline{\boldsymbol{X}}^{(13)2212}\right]$$

$$+\mathrm{i}\,\frac{1}{240}\left(\alpha_0(\boldsymbol{p})+\alpha_0(\boldsymbol{p}_0)\right)\left[72\overline{\boldsymbol{X}}^{(21)211}+90\overline{\boldsymbol{X}}^{(21)121}+18\overline{\boldsymbol{X}}^{(21)112}+138\overline{\boldsymbol{X}}^{(12)212}\right.$$

$$\left.+66\overline{\boldsymbol{X}}^{(12)122}+216\overline{\boldsymbol{X}}^{(12)221}+24\overline{\boldsymbol{X}}^{(30)}+120\overline{\boldsymbol{X}}^{(03)}\right]$$

$$-\frac{1}{240}(\alpha_0(\boldsymbol{p})+\alpha_0(\boldsymbol{p}_0))^2\left[312\overline{\boldsymbol{X}}^{(11)12}+516\overline{\boldsymbol{X}}^{(11)21}+749\overline{\boldsymbol{X}}^{(02)}+389\overline{\boldsymbol{X}}^{(20)}\right]$$

$$-\mathrm{i}\,\frac{1}{480}\left(\alpha_0(\boldsymbol{p})+\alpha_0(\boldsymbol{p}_0)\right)^3\left(1445\overline{\boldsymbol{X}}_u^{(1)}+1837\overline{\boldsymbol{X}}_d^{(1)}\right)\Big\},$$

(9)

4

4. The scattering matrices

When the expressions $\tilde{\boldsymbol{\Phi}}^{(nm)}$ are calculated we can deduce the scattering matrices $\overline{\boldsymbol{R}}^{(nm)}$. With the definition of the following integration operator $\mathcal{J}^{(n)}$

$$
\mathcal{J}^{(n)} = \int d^2\boldsymbol{r}\, d^2\boldsymbol{r'} \frac{d^2\boldsymbol{\xi}}{(2\pi)^2}\frac{d^2\boldsymbol{\xi'}}{(2\pi)^2}\frac{d^2\boldsymbol{\xi}_1}{(2\pi)^2}\cdots\frac{d^2\boldsymbol{\xi}_n}{(2\pi)^2}
$$
$$
\exp\left[-i(\boldsymbol{p}-\boldsymbol{p}_0-\boldsymbol{\xi})\cdot\boldsymbol{r} - i(\boldsymbol{p}-\boldsymbol{p}_0-\boldsymbol{\xi'})\cdot\boldsymbol{r'} - i(\alpha(\boldsymbol{p})+\alpha(\boldsymbol{p}_0))(h_1(\boldsymbol{r})+h_2(\boldsymbol{r'}))\right], \tag{10}
$$

we obtain the expressions:

$$
\begin{aligned}
\overline{\boldsymbol{R}}^{(10)}(\boldsymbol{p}|\boldsymbol{p}_0) &= \mathcal{J}^{(1)}\tilde{\boldsymbol{\Phi}}^{(10)}(\boldsymbol{p},\boldsymbol{p}_0,\boldsymbol{\xi}_1)h_1(\boldsymbol{\xi}_1)\\
\overline{\boldsymbol{R}}^{(01)}(\boldsymbol{p}|\boldsymbol{p}_0) &= \mathcal{J}^{(1)}\tilde{\boldsymbol{\Phi}}^{(01)}(\boldsymbol{p},\boldsymbol{p}_0,\boldsymbol{\xi}_1)h_2(\boldsymbol{\xi}_1)\\
\overline{\boldsymbol{R}}^{(11)}(\boldsymbol{p}|\boldsymbol{p}_0) &= \mathcal{J}^{(2)}\Big[\tilde{\boldsymbol{\Phi}}^{(11)12}(\boldsymbol{p},\boldsymbol{p}_0,\boldsymbol{\xi}_1,\boldsymbol{\xi}_2)h_1(\boldsymbol{\xi}_1)h_2(\boldsymbol{\xi}_2)\\
&\quad +\tilde{\boldsymbol{\Phi}}^{(11)21}(\boldsymbol{p},\boldsymbol{p}_0,\boldsymbol{\xi}_1,\boldsymbol{\xi}_2)h_2(\boldsymbol{\xi}_2)h_1(\boldsymbol{\xi}_1)\Big]\\
\overline{\boldsymbol{R}}^{(20)}(\boldsymbol{p}|\boldsymbol{p}_0) &= \mathcal{J}^{(2)}\tilde{\boldsymbol{\Phi}}^{(20)}(\boldsymbol{p},\boldsymbol{p}_0,\boldsymbol{\xi}_1,\boldsymbol{\xi}_2,\boldsymbol{\xi})h_1(\boldsymbol{\xi}_1)h_1(\boldsymbol{\xi}_2)\\
\overline{\boldsymbol{R}}^{(02)}(\boldsymbol{p}|\boldsymbol{p}_0) &= \mathcal{J}^{(2)}\tilde{\boldsymbol{\Phi}}^{(02)}(\boldsymbol{p},\boldsymbol{p}_0,\boldsymbol{\xi'},\boldsymbol{\xi}_1,\boldsymbol{\xi}_2)h_2(\boldsymbol{\xi}_1)h_2(\boldsymbol{\xi}_2)\\
\overline{\boldsymbol{R}}^{(21)}(\boldsymbol{p}|\boldsymbol{p}_0) &= \mathcal{J}^{(3)}\Big[\tilde{\boldsymbol{\Phi}}^{(21)112}(\boldsymbol{p},\boldsymbol{p}_0,\boldsymbol{\xi}_1,\boldsymbol{\xi}_2,\boldsymbol{\xi}_3)h_1(\boldsymbol{\xi}_1)h_1(\boldsymbol{\xi}_2)h_2(\boldsymbol{\xi}_3)\\
&\quad +\tilde{\boldsymbol{\Phi}}^{(21)121}(\boldsymbol{p},\boldsymbol{p}_0,\boldsymbol{\xi}_1,\boldsymbol{\xi}_2,\boldsymbol{\xi}_3)h_1(\boldsymbol{\xi}_1)h_2(\boldsymbol{\xi}_3)h_2(\boldsymbol{\xi}_2)\\
&\quad +\tilde{\boldsymbol{\Phi}}^{(21)211}(\boldsymbol{p},\boldsymbol{p}_0,\boldsymbol{\xi}_1,\boldsymbol{\xi}_2,\boldsymbol{\xi}_3)h_2(\boldsymbol{\xi}_3)h_1(\boldsymbol{\xi}_1)h_1(\boldsymbol{\xi}_2)\Big]\\
\overline{\boldsymbol{R}}^{(12)}(\boldsymbol{p}|\boldsymbol{p}_0) &= \mathcal{J}^{(3)}\Big[\tilde{\boldsymbol{\Phi}}^{(12)221}(\boldsymbol{p},\boldsymbol{p}_0,\boldsymbol{\xi}_1,\boldsymbol{\xi}_2,\boldsymbol{\xi}_3)h_2(\boldsymbol{\xi}_1)h_2(\boldsymbol{\xi}_2)h_1(\boldsymbol{\xi}_3)\\
&\quad +\tilde{\boldsymbol{\Phi}}^{(12)212}(\boldsymbol{p},\boldsymbol{p}_0,\boldsymbol{\xi}_1,\boldsymbol{\xi}_2,\boldsymbol{\xi}_3)h_2(\boldsymbol{\xi}_1)h_1(\boldsymbol{\xi}_3)h_2(\boldsymbol{\xi}_2)\\
&\quad +\tilde{\boldsymbol{\Phi}}^{(12)122}(\boldsymbol{p},\boldsymbol{p}_0,\boldsymbol{\xi}_1,\boldsymbol{\xi}_2,\boldsymbol{\xi}_3)h_1(\boldsymbol{\xi}_3)h_2(\boldsymbol{\xi}_1)h_2(\boldsymbol{\xi}_2)\Big]\\
\overline{\boldsymbol{R}}^{(30)}(\boldsymbol{p}|\boldsymbol{p}_0) &= \mathcal{J}^{(3)}\tilde{\boldsymbol{\Phi}}^{(30)}(\boldsymbol{p},\boldsymbol{p}_0,\boldsymbol{\xi}_1,\boldsymbol{\xi}_2,\boldsymbol{\xi}_3)h_1(\boldsymbol{\xi}_1)h_1(\boldsymbol{\xi}_2)h_1(\boldsymbol{\xi}_3)\\
\overline{\boldsymbol{R}}^{(03)}(\boldsymbol{p}|\boldsymbol{p}_0) &= \mathcal{J}^{(3)}\tilde{\boldsymbol{\Phi}}^{(03)}(\boldsymbol{p},\boldsymbol{p}_0,\boldsymbol{\xi}_1,\boldsymbol{\xi}_2,\boldsymbol{\xi}_3)h_2(\boldsymbol{\xi}_1)h_2(\boldsymbol{\xi}_2)h_2(\boldsymbol{\xi}_3).
\end{aligned} \tag{11}
$$

5. The bistatic cross-sections

To compute the bistatic cross-section, we take the expansion of $\overline{\boldsymbol{R}}$ in terms of the (mn) scattering matrices given by $\overline{\boldsymbol{R}}^{(nm)}$. The incoherent bistatic cross-section is given by:

$$
\overline{\boldsymbol{\gamma}}_{ij}^{incoh}(\boldsymbol{p}|\boldsymbol{p}_0) = \frac{K_0^2\cos^2\theta}{A\,(2\pi)^2\cos\theta_0}\left[<\overline{\boldsymbol{R}}(\boldsymbol{p}|\boldsymbol{p}_0)\odot\overline{\boldsymbol{R}}(\boldsymbol{p}|\boldsymbol{p}_0)> - <\overline{\boldsymbol{R}}(\boldsymbol{p}|\boldsymbol{p}_0)>\odot<\overline{\boldsymbol{R}}(\boldsymbol{p}|\boldsymbol{p}_0)>\right], \tag{12}
$$

where the angle brackets denote an average over the ensemble of realizations of the functions $h_i(r)$, and ij are the polarization components.

An example of contribution coming from $4h_2$ heights reads:

$$
< \overline{\boldsymbol{R}}^{(03)}(\boldsymbol{p}|\boldsymbol{p}_0) \odot \overline{\boldsymbol{R}}^{(01)}(\boldsymbol{p}|\boldsymbol{p}_0) > = \exp^{\left[-(\alpha_0(\boldsymbol{p})+\alpha_0(\boldsymbol{p}_0))^2/2W_{22}(0)\right]} \times
$$

$$
\int d^2\boldsymbol{x}_1\, d^2\boldsymbol{x}_2 \exp^{\left[-\mathrm{i}(\boldsymbol{p}-\boldsymbol{p}_0)(\boldsymbol{x}_1-\boldsymbol{x}_2)\right]} \exp^{\left[(\alpha_0(\boldsymbol{p})+\alpha_0(\boldsymbol{p}_0))^2 W_{22}(\boldsymbol{x}_1-\boldsymbol{x}_2)\right]} \times
$$

$$
\int \frac{\mathrm{d}^2\boldsymbol{\xi}}{(2\pi)^2}\, \exp^{\left[\mathrm{i}\boldsymbol{\xi}(\boldsymbol{x}_1-\boldsymbol{x}_2)\right]} W_{22}(\boldsymbol{\xi}) \int \frac{\mathrm{d}^2\boldsymbol{\xi}_2}{(2\pi)^2}\, W_{22}(\boldsymbol{\xi}_2) \left[\overline{\boldsymbol{\Phi}}^{(03)}(\boldsymbol{p},\boldsymbol{p}_0,\boldsymbol{\xi},\boldsymbol{\xi}_2,-\boldsymbol{\xi}_2) \odot \overline{\boldsymbol{\Phi}}^{(01)\,*}(\boldsymbol{p},\boldsymbol{p}_0,\boldsymbol{\xi}) \right.
$$

$$
+ \overline{\boldsymbol{\Phi}}^{(03)}(\boldsymbol{p},\boldsymbol{p}_0,\boldsymbol{\xi}_2,\boldsymbol{\xi},-\boldsymbol{\xi}_2) \odot \overline{\boldsymbol{\Phi}}^{(01)\,*}(\boldsymbol{p},\boldsymbol{p}_0,\boldsymbol{\xi})
$$

$$
\left. + \overline{\boldsymbol{\Phi}}^{(03)}(\boldsymbol{p},\boldsymbol{p}_0,\boldsymbol{\xi}_2,-\boldsymbol{\xi}_2,\boldsymbol{\xi}) \odot \overline{\boldsymbol{\Phi}}^{(01)\,*}(\boldsymbol{p},\boldsymbol{p}_0,\boldsymbol{\xi}) \right] , \tag{13}
$$

where we have assumed a Gaussian expression for the heights in our applications, and W_{ij} are the correlation functions associated with the surfaces.

6. An illustrative structure and conclusions

As an application of the previous formalism we consider a slab made of a air-dielectric film whose dielectric constant is $\epsilon_1 = 2.6896 + i0.0075$, deposited on a silver surface with $\epsilon_2 = -18.3 + i0.55$. The air-dielectric interface is a two-dimensional rough surface, whose parameters are $\sigma_1 = 15$nm and $l_1 = 100$nm.
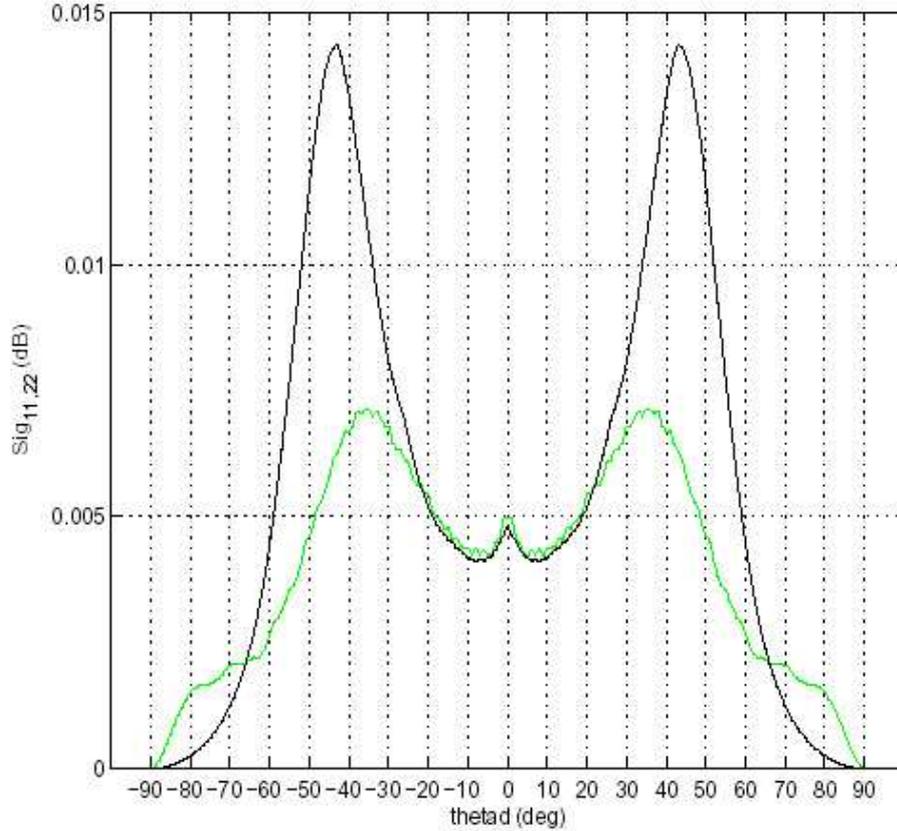

FIG. 2. *Diffuse scattering cross-section for a normal incident wave in the incidence plane. Polarization TE-TE black curve, polarization TM-TM green curve.*

We consider that the randomly rough surfaces are Gaussian surfaces with Gaussian auto-correlation functions . The dielectric-silver boundary has a roughness defined by $\sigma_2 = 5$nm and $l_2 = 100$nm. The mean thickness of the dielectric layer is constant and equal to 500nm. The incident wave has an arbitrary polarization and its wavelength is $\lambda = 632.8$nm. We show in figure 2 the incoherent bistatic cross-section for different polarizations. We have checked that when the orders increase the magnitudes of the corresponding contributions decrease justifying a posteriori a perturbative development, however there is no proof of convergence for the series. In figure 2, we observe the backscattering enhancement at $\theta_d = 0\,^\circ$.

We have studied structures with two-dimensional randomly rough surfaces. We can apply this formalism to electromagnetic wave scattering from freestanding films or films on a substrate, where one or both of those surfaces are randomly rough. In this paper, we have discussed the extension of the small-slope approximation method to randomly rough slabs. The fourth order term of the perturbative development is included in the formalism. We have calculated the perturbative development for different structures composed of two randomly rough surfaces separating homogeneous medium. The numerical results show an enhancement of the backscattering for the structure we have presented. We have focused on less-known mechanisms that occur in the cases where the randomly rough surfaces enclose bounded structures. These mechanisms are included in the extension of the small-slope approximation. We have obtained a general formulation which can be applied to configurations including slab with randomly rough surfaces.

This analysis is relevant to problems of laser cross-section calculation, remote sensing of irregular layered structures and remote detection of chemical coatings.

References

1. A. G. Voronovich, *Wave Scattering from Rough Surfaces*. Springer-Verlag, Berlin, (1994).
2. A. G. Voronovich, "Small-Slope Approximation for Electromagnetic Wave Scattering at a Rough Interface of Two Dielectric Half-Spaces", *Waves in Random Media*, Vol. 4 , pp 337367, 1994.
3. G. Berginc and B. Chevalier, "Small-Slope Approximation Method: Scattering of a Vector Wave from 2D Dielectric and Metallic Surfaces with Gaussian and Non Gaussian Statistics", in T. C. Philip Zu-Han Gu, and A. A. Maradudin editors, *SPIE*, Vol. 4100, *Scattering and Surface Roughness III*, pp 2232, 2000.
4. G. Berginc, "Small-Slope Approximation Method: A Further Study of Vector Wave Scattering from TwoDimensional Surfaces and Comparison with Experimental Data", in *Progress in Electromagnetic Research* (J.A. Kong ed.), Vol. 37, pp 251-287, EMW Publishing, 2003.
5. A. Soubret, G. Berginc and C Bourrely, "Application of Reduced Rayleigh Equations to Electromagnetic Wave Scattering by Two-dimensional Randomly rough Surfaces", *Physical Review B*, Vol. 63, pp 245411-245431, June 2001.
6. G. Berginc and C. Bourrely, "Scattering of an Electromagnetic Wave from 3-D Rough Layers: SmallAmplitude Method and Small-Slope Approximation", *Progress In Electromagnetic Research Symposium*, Cambridge, USA, 2006.